Structural Characterization of *N*-Methylpyridoxine (MePN; PN = Vitamin B_6) and Its Diorganotin Complexes [SnR_2(MePN-H)]I (R = Me, Et, Bu and Ph)

José S. Casas,[a] Alfonso Castiñeiras,[a] Félix Condori,[a] María D. Couce,[b] Umberto Russo,[c] Agustín Sánchez,[a] José Sordo,*[a] and José M. Varela[a]

Keywords: Vitamins / Tin / IR spectroscopy / Mössbauer spectroscopy / NMR spectroscopy

For comparison with the corresponding pyridoxine complexes we have prepared dimethyl-, diethyl-, dibutyl- and diphenyltin(IV) complexes of *N*-methylpyridoxine (MePN). The compounds [$SnMe_2$(MePN–H)]I (**1**), [$SnEt_2$(MePN–H)]I (**2**), [$SnBu_2$(MePN–H)]I (**3**) and [$SnPh_2$(MePN–H)]I·H_2O (**4**) were isolated and characterized by IR, Raman, Mössbauer, ^1H, ^{13}C and ^{119}Sn NMR spectroscopy, and by EI and FAB mass spectrometry. The crystal structures of [HMePN]I and of compounds **1**, **2**·2H_2O and **3** were determined by X-ray diffractometry. Their lattices contain dimeric [SnR_2-(MePN–H)]$_2^{2+}$ units (R = Me, Et, Bu) in which two bridging-chelating methylpyridoxinato anions link pentacoordinate Sn atoms with coordination polyhedra closer to square pyramids than to trigonal bipyramids. NMR results show that the dimeric cations persist in $(CD_3)_2SO$.

Introduction

As part of our research on the interaction of diorganotin compounds with vitamins and derivatives,[1,2] we have described the interaction of pyridoxine (PN, vitamin B_6) with dimethyltin(IV) and diethyltin(IV) cations in water/ethanol mixtures in the presence of biologically relevant anions such as Cl^- and NO_3^- in various molar ratios.[3,4] These reactions led to complexes containing mono- or di-deprotonated pyridoxine ligands ([PN−H] and [PN−2H], respectively) in dimeric [SnR_2(PN−H)]$_2^{2+}$ or [SnR_2(PN−2H)]$_2$ units. In these species (**I**, **II**) the tin centre was usually pentacoordinated to the two R groups, the deprotonated phenolic oxygen atom of one PN molecule and the deprotonated 4-(hydroxymethyl) oxygen atoms of this and another PN molecule, the latter oxygen atoms bridging the tin atoms of each dimer. In some dimethyltin derivatives the tin atom was hexacoordinate owing to an additional bond with the 5-(hydroxymethyl) group of a neighbouring dimer or with a water molecule.

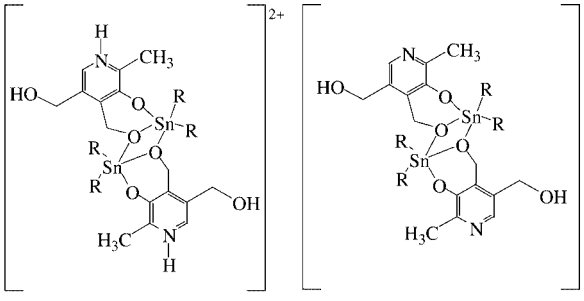

I **II**

N-Methylation suppresses the normal biological activity of PN[5] and methylation of its 4-(hydroxymethyl) group makes it toxic.[6] To find out whether *N*-methylation also significantly affects its coordination to diorganotin cations, in this work we have determined the structures of [HMePN]I and of the complexes resulting from its reaction with SnR_2O (R = Me, Et, Bu), and compared them with those of PN and its diorganotin complexes.

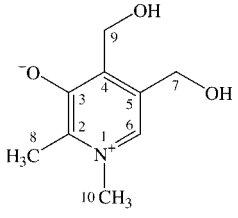

III

[a] Departamento de Química Inorgánica, Facultade de Farmacia, Universidade de Santiago de Compostela,
15782 Santiago de Compostela, Galicia, Spain
Fax: (internat.) + 34-981/594912
E-mail: qijsordo@usc.es
[b] Departamento de Química Inorgánica, Facultade de Ciencias, Universidade de Vigo,
36200 Vigo, Galicia, Spain
[c] Dipartimento di Chimica Inorganica, Metallorganica ed Analitica, Università di Padova,
Padova, Italy

  DOI: 10.1002/ejic.200200631

We first attempted to use [HMePN]I to prepare *N*-methylpyridoxine [MePN (**III**)] with a view to treating the latter with the diorganotin oxides in reactions that parallel those previously[7] carried out with PN. However, since the resistance of MePN to deprotonation caused its reaction with SnR_2O to afford mainly impure MePN, we eventually treated the oxides (R = Me, Et, Bu and Ph) with PN and methyl iodide in a one-pot synthesis. This afforded the complexes $[SnMe_2(MePN-H)]I$, $[SnEt_2(MePN-H)]I$, $[SnBu_2(MePN-H)]I$ and $[SnPh_2(MePN-H)]I\cdot H_2O$, the first three of which were characterized, as with [HMePN]I, by single-crystal X-ray diffractometry. This appears to be the first study of MePN complexes and the first structural study of MePN.

Results and Discussion

Synthesis

The four complexes $[SnR_2(MePN-H)]I$ were prepared by adding solid SnR_2O and methyl iodide to a solution of pyridoxine in toluene/ethanol (Scheme 1). Compounds **1** and **3** crystallized as such from methanol, but compound **2** acquired two H_2O molecules during crystallization.

$$SnR_2O + PN + MeI \xrightarrow[-H_2O]{\text{toluene/ethanol}} [SnR_2(MePN\text{–}H)]I$$

R = Me (**1**)
Et (**2**)
Bu (**3**)
Ph (**4**)

Scheme 1

Description of the Structures

[HMePN]I

Figure 1 shows the structure of [HMePN]I together with the numbering scheme used. Selected distances and angles are listed in Table 1. The crystal is composed of $[HMePN]^+$ cations and iodide anions. In the cation the pyridine ring is planar and C(7), C(8), C(9), O(2) and O(3) are close to this plane, while C(10) and O(1) lie farther away.

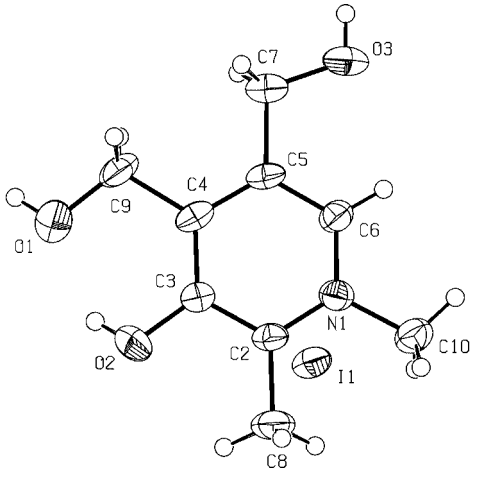

Figure 1. Crystal structure of [HMePN]I, showing the numbering scheme

Although limited by the high e.s.d.s, a comparison of bond lengths with those found for PN[8] shows that *N*-methylation and protonation do not change the ring parameters very much, even for bonds involving or close to the N atom; the most affected bond, C(3)−O(2), is shortened from 1.374(4) to 1.348(10) Å. Such changes are similar, bearing in mind the high e.s.d.s, to those caused by *N*-protonation, as observed in HPNCl[9] [except, of course, for N(1)−C(10)]. The bond angle most affected by *N*-methylation or protonation is C(2)−N(1)−C(6) [119.3(3), 123.8(5) and 122.4(7)° in PN, HPNCl and [HMePN]I, respectively].

As in HPNCl,[9] the O(2) atom of the phenolic hydroxy group and the O(1) atom of the $C(4)-CH_2OH$ group are linked by an intramolecular hydrogen bond [0.82, 1.84 and 2.512(5) Å; 138.1°], which, by pulling O(1) out of the ring plane, is responsible for the different arrangements of the $C(4)-CH_2OH$ and $C(5)-CH_2OH$ groups. Each CH_2OH group is also involved in a structure-stabilizing intramolecular hydrogen bond with a neighbouring iodide ion [O(1)−H(1)···I(1)$^{\#1}$: 0.82, 2.71 and 3.423(6) Å, 146.3°; O(3)−H(3)···I(1)$^{\#2}$: 0.82, 2.86 and 3.593(8) Å, 150.0°; #1: $x + 1/2, -y + 3/2, z + 1/2$; #2: $-x, -y + 1, -z + 2$].

[SnMe$_2$(MePN−H)]I (1)

The dimethyltin derivative consists of dimeric $[SnMe_2(MePN-H)]_2^{2+}$ units and iodide ions. Figure 2 shows the structure of the dimeric unit and the numbering scheme used. Selected distances and angles are listed in Table 1.

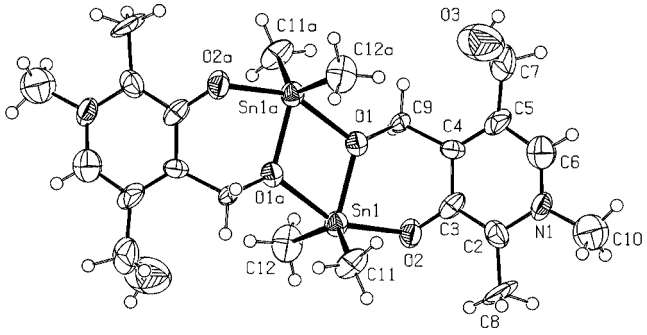

Figure 2. Crystal structure of the cation in the complex $[SnMe_2(MePN-H)]I$ (**1**), showing the numbering scheme (a: $-x, -y + 1, -z$)

In the dimeric unit the two methylpyridoxinato ligands bridge the tin atoms with their deprotonated C(4) substituents. Each tin atom coordinates to two methyl C atoms, to the deprotonated O(2) and O(1) atoms of one methylpyridoxinato ligand and to the similarly deprotonated O(1) atom of the other. As τ[10] = 0.35 for the coordination polyhedron, it is closer to a square pyramid, with the "foreign" O(1) apical, than to a trigonal bipyramid.

In the central Sn_2O_2 ring the length of one Sn−O bond, Sn−O(1), like that of Sn−O(2), is slightly less than the sum

Table 1. Selected bond lengths [Å] and angles [°] in [HMePN]I, **1**, **2**·2H_2O and **3**, with e.s.d.s in parentheses; symmetry operations (#1): for **1**: $-x, -y + 1, -z$; for **2**·2H_2O: $-x + 1, -y + 1, -z$, for **3**: $-x + 3/2, -y, -z - 1/4$

	[HMePN]I	**1**	**2**·2H_2O	**3**
(a) Tin environment:				
Sn(1)−O(1)		2.060(9)	2.080(4)	2.171(5)
Sn(1)−O(2)		2.068(10)	2.119(4)	2.119(5)
Sn(1)−C(11)		2.090(13)	2.116(7)	2.130(8)
Sn(1)−C(12)		2.096(15)	2.117(7)	2.109(8)
Sn(1)−O(1)$^{\#1}$		2.231(9)	2.295(4)	2.073(5)
Sn(1)−Sn(1)$^{\#1}$		3.549(3)	3.5815(9)	3.5595(16)
O(1)−Sn(1)−C(11)		112.9(5)	108.1(2)	103.5(3)
O(1)−Sn(1)−C(12)		113.0(5)	104.2(2)	109.2(3)
O(1)−Sn(1)−O(2)		84.4(4)	83.20(15)	84.38(18)
O(1)−Sn(1)−O(1)$^{\#1}$		68.4(4)	70.20(16)	70.04(19)
O(2)−Sn(1)−C(11)		99.6(6)	95.1(2)	96.8(3)
O(2)−Sn(1)−C(12)		98.7(6)	99.4(3)	92.5(3)
O(2)−Sn(1)−O(1)$^{\#1}$		152.8(4)	153.21(15)	154.34(17)
C(11)−Sn(1)−C(12)		131.8(7)	145.9(3)	146.7(3)
C(11)−Sn(1)−O(1)$^{\#1}$		91.2(5)	90.3(2)	91.4(3)
C(12)−Sn(1)−O(1)$^{\#1}$		92.3(5)	90.3(3)	94.0(3)
(b) Pyridoxine ligand:				
O(1)−C(9)	1.405(11)	1.439(15)	1.436(7)	1.431(8)
C(4)−C(9)	1.506(11)	1.509(19)	1.512(8)	1.504(9)
C(3)−C(4)	1.383(11)	1.400(19)	1.397(8)	1.415(9)
C(3)−O(2)	1.348(10)	1.329(18)	1.328(6)	1.318(8)
N(1)−C(2)	1.333(11)	1.375(19)	1.352(7)	1.369(8)
N(1)−C(6)	1.348(11)	1.343(19)	1.355(8)	1.315(9)
O(1)−C(9)−C(4)	110.6(8)	110.6(11)	110.8(5)	111.9(6)
C(3)−C(4)−C(9)	123.6(9)	114.6(14)	117.2(5)	119.5(6)
C(5)−C(4)−C(3)	117.7(8)	121.9(16)	119.4(5)	118.9(6)
C(5)−C(4)−C(9)	118.7(8)	123.5(14)	123.3(5)	121.7(6)
O(2)−C(3)−C(4)	124.0(8)	122.9(14)	121.6(5)	120.9(7)
O(2)−C(3)−C(2)	115.2(7)	118.6(14)	118.8(5)	118.7(7)
C(2)−C(3)−C(4)	120.8(8)	118.5(16)	119.5(5)	120.2(6)

of the covalent radii of Sn and O (2.13 Å),[11] whereas that of the other, Sn−O(1)^a, is slightly larger [2.231(9) Å]. The parameters of this ring are similar to those in other dimeric compounds with rings based on O-bridges.[12] The ring is planar, and makes an angle of 46.26° with the pyridine rings of the [MePN−H] ligands, which are, likewise, practically planar (r.m.s. deviation = 0.0160 Å).

Although the structural parameters of $[HMePN]^+$ change upon double deprotonation and coordination, the high e.s.d.s hinder rigorous analysis of the smaller changes, such as those undergone by the C(9)−O(1) and C(3)−O(2) bonds involving the coordinating oxygen atoms. However, the C(3)−C(4)−C(9) angle narrows significantly from 123.6(9)° in [HMePN]I to 114.6(14)° in **1** due to formation of the SnO(2)C(3)C(4)C(9)O(1) chelate ring.

The iodide ion is hydrogen-bonded to the noncoordinating hydroxymethyl group, C(5)−CH_2OH [O(3)−H(3)···I(1)$^{\#2}$: 0.82, 2.75 and 3.517(15) Å, 157.0°; #2: $x, -y + 1/2, z - 1/2$].

Comparison of this structure with those[3] of [$SnMe_2$(PN−H)]NO_3·2H_2O and [$SnMe_2$(H_2O)(PN−H)]Cl·H_2O, which like **1** are composed of dimeric units, reveals similar central Sn_2O_2 rings [although Sn−O(2) is shorter in **1**] but their tin environments are different, the PN−H derivatives being hexacoordinate. They also have different hydrogen-bond networks.

[$SnEt_2$(MePN−H)]I·2H_2O (2·2H_2O)

The diethyltin derivative consists of [$SnEt_2$(MePN−H)]$_2^{2+}$ units, iodide ions and water molecules. Figure 3 shows the structure of the dimeric unit and the numbering scheme used. Selected distances and angles are listed in Table 1.

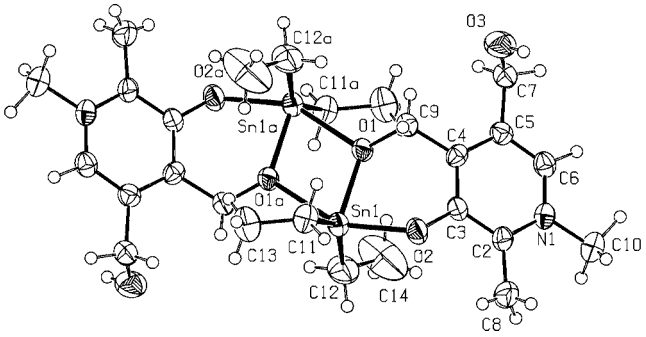

Figure 3. Crystal structure of the cation in the complex [$SnEt_2$(MePN−H)]I·2H_2O (**2**·2H_2O), showing the numbering scheme (a: $-x + 1, -y, -z + 1$)

The essential structural features of the dimeric unit are, as in **1**, a central Sn_2O_2 ring and the two methylpyridoxinato ligands linked to this ring. However, the following differences deserve comment.

In the Sn_2O_2 ring, the Sn−O bonds are longer in **2**·$2H_2O$ than in **1**, so that even though the Sn−O(1)−Sn^i angle is narrower in **2**·$2H_2O$ than in **1** [109.80(16)° as against 111.6(4)°] the two tin atoms are separated by a greater distance in **2**·$2H_2O$ [3.5815(9) Å] than in **1**. The coordination polyhedron is closer to a square pyramid in **2**·$2H_2O$ than in **1** (τ = 0.12 versus 0.35), mainly because the C−Sn−C angle is wider in **2**·$2H_2O$ than in **1** [145.9(3)° versus 131.8(7)°]. The dihedral angles between the planar Sn_2O_2 ring and the practically planar pyridine rings (r.m.s. deviation = 0.0073 Å) are narrower in **2**·$2H_2O$ than in **1** (33.86° as against 46.26°).

The main difference in crystal packing between **1** and **2**·$2H_2O$ is the presence in **2** of a denser network of hydrogen bonds involving the iodide ion, the water molecules, and the C(5)−CH_2OH group [O(4)−H(4B)···I(1): 1.00(8), 2.52(8) and 3.501(7) Å, 168(6)°; O(4)−H(4A)···O(3)$^{\#2}$: 0.98(8), 2.33(9) and 2.839(9) Å, 112(7)°; O(3)−H(3)···O(4)$^{\#3}$: 0.82, 2.27 and 2.839(9) Å, 126.4°; #2: x, $-y$ + 1/2, z + 1/2; #3: x, $-y$ + 1/2, z − 1/2].

The structure of **2**·$2H_2O$ is very similar to that of $[SnEt_2(PN-H)]NO_3 \cdot 2H_2O$.[3] In particular, the Sn_2O_2 rings are practically identical. The most noteworthy differences are the shorter Sn−C bonds of **2**·$2H_2O$ and its narrower C−Sn−C angles [145.9(3)° versus 152.77(13)°].

[SnBu$_2$(MePN−H)]I (3)

The dibutyltin derivative consists of dimeric $[SnBu_2(MePN-H)]_2^{2+}$ units and iodide ions. Figure 4 shows the structure of the dimeric unit (for clarity the butyl carbon atoms are reduced in size) and the numbering scheme used. Selected distances and angles are listed in Table 1.

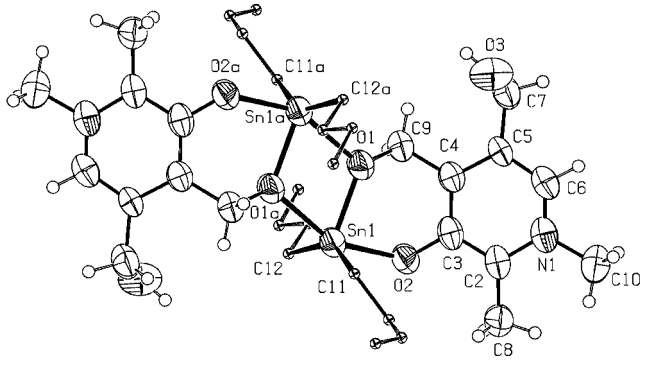

Figure 4. Crystal structure of the cation in the complex $[SnBu_2(MePN-H)]I$ (**3**), showing the numbering scheme; for clarity the butyl carbon atoms are reduced in size (a: $-x$, $-y$, $-z$)

The dimeric unit has a similar structure to **1** and **2**·$2H_2O$, its bond lengths and angles differing only very slightly from those of **2**·$2H_2O$. The Sn−O(1)^a distance is slightly shorter in **3**, but the tin environment has a similar degree of distortion. The hydrogen-bond network in **3** is practically identical to that of **1** [O(3)−H(3)···I(1)$^{\#2}$: 0.82, 2.56 and 3.372(6) Å, 172.4°; #2: x − 1/2, $-y$ + 1/2, $-z$ + 1/2].

Conversely, the angle between the planar Sn_2O_2 ring and each of the practically planar py rings (r.m.s. deviation = 0.0082 Å) is only 29.26° in **3**, falling from 46.26° for R = Me and 33.86° for R = Et, possibly due to the increasing bulk of R.

Vibrational Spectra

In addition to those given in the Exp. Sect., the IR spectrum of [HMePN]I exhibits bands at 3429, 3344, 3249 and 3150 cm^{-1}, attributed to stretching vibrations of the three OH groups. Deprotonation to [MePN] clears the IR spectrum in this region, leaving one broad band at 3160 cm^{-1} and another band at 3101 cm^{-1}, owing to the absence of phenolic ν(OH) and to alteration of the hydrogen-bonding network, which must likewise be responsible for the appearance of a broad medium-strong band at 2850 cm^{-1}.

The ν(C−O) bands for the C(4)- and C(5)−CH_2OH groups[13] of the complexes (see Exp. Sect.) are, like the vibrations of the pyridine ring, close to those of MePN. Near 1300 cm^{-1} the complexes show a strong IR band (medium in the Raman spectra) that is attributed[14] to ν(C−O) of the coordinated phenolic group.

For the methyl and ethyl derivatives the ν_{asym}(Sn−C) and ν_{sym}(Sn−C) vibrations are present in both the IR and Raman spectra, as expected for a nonlinear C−Sn−C fragment. Their positions are close to those[3,4] of unmethylated pyridoxine complexes.

Mössbauer Spectra

The Mössbauer spectra, recorded at 80 K, consist of well-resolved, slightly asymmetric doublets with isomer-shift and quadrupole-splitting values that are consistent with penta coordination around the tin(IV) centre. As usual, the isomer shifts increase on going from the methyl to the butyl derivative, while the diphenyl compound has a lower value due to its different electronegativity. Because of the marked distortion of the complexes from ideal trigonal-bipyramidal geometry, only the contributions of the covalently bonded organic groups were used in calculating Q.S. by means of the point charge model and the simplified formula[15] Q.S. = $-4[R](1-3/4\ \sin^2\ \theta)^{1/2}$. Using the experimental C−Sn−C bond angles, the Q.S. values are quite close to the experimental ones whether the p.q.s. is taken as −0.94 mm/s (valid for organic moieties in tba positions) or −1.13 mm/s (typical of tbe positions). The fact that the experimental Q.S. value of the diphenyl derivative is much lower than those calculated for the dialkyl derivatives suggests that it is even more strongly distorted.

Only the data for the diethyltin derivative can be compared with those of the corresponding PN complex,[3] the dimethyltin derivative of PN being hexacoordinate. The isomer shifts of $[SnEt_2(PN-H)]NO_3 \cdot 2H_2O$ and $[SnEt_2(PN-H)]Cl$, 1.63 and 1.61, respectively, are larger than the 1.49 found for $[SnEt_2(MePN-H)]I$, and as the iso-

mer shift reflects the s-electron density at the tin nucleus, this suggests that MePN−H has less donor ability than PN−H (vide infra).

NMR Spectroscopy

^{1}H, ^{13}C and ^{119}Sn NMR spectroscopic data recorded in [D_6]DMSO solution, and solid-state ^{13}C CP MAS NMR spectroscopic data, are given in the Exp. Sect.

a) Solid State

Satisfactory ^{13}C CP MAS spectra were obtained for all compounds except the diphenyltin complex. Most carbon atoms afforded separate signals, which were assigned on the basis of previously reported data for similar compounds[3,7c] and on the results of solution studies (see below). *N*-Methylation of PN shifted the C(3) signal ca. 10 ppm downfield. The C(6) and C(4) signals were also deshielded (but to a lesser extent), and the other carbon atoms were shielded, especially C(5) and C(8). This re-distribution of charge in the ring must have a substantial effect on the C(3)−O(2) bond and the charge on the potential donor atom O(2). Protonation of O(2) upon formation of [HMePN]I shielded C(3) by ca. 10 ppm, and C(2), C(6) and C(4) less markedly, while the other carbon atoms were deshielded [C(5) by ca. 9 ppm and the others by ca. 3 ppm]. These results, the X-ray data and the fact that protonation of O(2) in PN to give PN·H$^+$ shifts the C(3) signal slightly downfield (from δ = 151.4 to 153.4 ppm[3]) suggest that *N*-methylation of PN increases the order of the C(3)−O(2) bond, which should affect the donor ability of O(2).

The ^{13}C NMR spectra of the ligand after deprotonation and coordination to the organometallic moieties are very similar, indicating that, as found in the X-ray study of **1**−**3**, they all have the same coordination mode. As in the PN analogues,[3] C(3) and C(4) are deshielded and all other carbon atoms are shielded.

At high field, the spectra show signals corresponding to the organometallic moieties. Compound **1** gives two peaks for the dimethyltin carbon atoms, one at a position similar to that observed in solution (vide infra), δ = 5.6 ppm, and the other slightly upfield at δ = 1.8 ppm, showing the methyl groups to be magnetically different. Similarly, the spectrum of compound **3** shows seven peaks instead of the four found in solution, in keeping with the high anisotropy exhibited by this compound in the X-ray study.

b) Solution

The published ^{1}H NMR data for the PN analogues[3,4] contain an error: the position of the H(6) signal being reported as δ = 8.17 ppm instead of δ = 7.88 ppm. In the present study, methylation of PN markedly shielded H(6), and to a lesser extent the C(9)H_2 and C(7)H_2 protons, and deshielded the C(8)H_3 protons and H(O3). ^3J for the coupling of H(O3) with C(7)H_2 is now 5.2 Hz as against 5.8 Hz in PN. The H(O2) signal was not located, the high acidity of this OH group probably resulting in fast exchange with the deuterium atoms of the solvent. In [HMePN]I, in which MePN is protonated, all the protons are deshielded with respect to MePN, especially H(6) (by 1.07 ppm).

Coordination to SnR_2^{2+} shielded all the protons of [HMePN]I except C(9)H_2, which were slightly deshielded. Flanking the C(9)H_2 singlet in the spectra of **1**, **2** and **3** were satellites corresponding to coupling between these protons and ^{119}Sn, showing that the interaction between O(1) and the tin atoms observed in the solid state persists in solution. The absence of satellites around the signal at δ ≈ 4.5 ppm, assigned to C(7)H_2, rules out interaction between O(3) and the metal atom.

The chemical shifts of the organometallic fragments are similar to those found[3,4,7c] for tin complexes in [D_6]DMSO. Substitution of the ^2J(^{1}H-^{119}Sn) value of **1** (87.0 Hz) in Equation (2) of Lockhart and Manders'[16] study of dimethyltin compounds predicts a C−Sn−C angle of 140°; this is wider than that observed in the X-ray study (131.8°) which may be due to interaction with the solvent.

The chemical shifts of the ligand carbon atoms agree well with the ^{13}C CP-MAS data (taking into account the breadth of the CP-MAS signals). This suggests that the MePN ligand has the same stereochemistry in both states.

^1J(^{13}C-^{119}Sn) constants were only measurable for **1** and **3**. The value for **3** is in the range 500−700 Hz, found[17] for other five-coordinate diorganotin complexes. That of the methyl derivative is outside this range, but also outside the 800−1000 Hz range found[17] for hexacoordinate compounds. When the value for **1** is substituted into Lockhart and Manders' equation,[18] a C−Sn−C angle of 145° is obtained, which is 5° wider than that obtained using the ^2J value but, likewise, suggests that the angle is widened due to the effect of the solvent. By contrast, substitution of ^1J(^{13}C-^{119}Sn) of **3** in the relationship obtained by Holecek et al.[19] for dibutyltin compounds predicts a C−Sn−C angle of 141°, close to the 146.7° observed in the solid state and indicative of the persistence of pentacoordination in solution. The bulky butyl groups may prevent incorporation of the solvent in **3**.

The single ^{119}Sn resonance of the complexes shows that they each have only one type of organotin moiety. Although ^{119}Sn chemical shifts are influenced by several factors,[20] the coordination number of the tin atom is one of the most important:[21] our compounds show a very narrow range, δ = −170.2 to −233.5 ppm, which is within that reported for pentacoordinate organotin compounds.[17,21,22]

Experimental Section

Material and Methods: Pyridoxine (Aldrich), methyl iodide (Aldrich), silver carbonate (Aldrich), dimethyltin oxide (Alfa) and dibutyltin oxide (Aldrich) were used as received. Diethyl- and diphenyltin oxides were obtained by treating the corresponding chlorides with sodium hydroxide. Elemental analyses were performed with a Fisons 1108 microanalyser. Melting points were determined with a Büchi Dr. Tottoli apparatus and are uncorrected. The conductivities of 10^{-3} M solutions in DMF were measured with a Crison MicroCM2202 conductivity meter. Mass spectra were recorded with a Kratos MS50TC spectrometer connected to a DS90 system,

operating under either EI conditions (direct insertion probe, 70 eV, 250 °C) or in FAB mode (*m*-nitrobenzyl alcohol, Xe, 8 eV; ca. 1.28 × 10^{-15} J); ions were identified by DS90 software and the data characterizing the metallated peaks were calculated using the isotope ^{120}Sn. IR spectra (KBr pellets or Nujol mulls) and Raman spectra (polycrystalline samples) were recorded with a Bruker IFS66V FT-IR spectrometer equipped with an FRA-106 Raman accessory and are reported below using the following abbreviations: vs = very strong, s = strong, m = medium, w = weak, sh = shoulder, br = broad. Mössbauer spectra were recorded at 80.0 K in a Harwell cryostat; the $Ca^{119m}SnO_3$ source (15 mCi, NEN) was kept at room temperature and moved with a triangular velocity wave form; suitable computer programs were employed to fit Lorentzian lineshapes to the experimental data. Solid-state NMR spectra were recorded with a Bruker AMX 300 spectrometer at 75.40 MHz using 7-mm o.d. zirconia rotors and the standard Bruker CPTOSS or CP_2LEV pulse programs at 3 and 4 kHz spinning speeds, a contact time of 1 ms and a recycle delay of 5 s; linewidths varied between 100 and 200 Hz, and chemical shifts are referred to glycine (δ = 176.3 ppm). ^{1}H and ^{13}C NMR spectra in solution were recorded at room temperature with a Bruker AMX 300 operating at 300.14 and 75.40 MHz, respectively, by using 5-mm o.d. tubes; chemical shifts are reported relative to TMS using the solvent signal [δ(^{1}H) = 2.50 ppm; δ(^{13}C) = 39.5 ppm] as reference. ^{119}Sn NMR spectra were recorded at 186.50 MHz with a Bruker AMX 500 spectrometer by using 5-mm o.d. tubes and are reported relative to external neat $Sn(CH_3)_4$. Elemental analyses, mass, IR, Raman and NMR spectra and X-ray data were obtained at CACTUS, University of Santiago de Compostela.

Synthesis of [HMePN]I and MePN

[HMePN]I: This compound was prepared by a published procedure[23] as follows. Methyl iodide (8 mL) was added to a solution of pyridoxine (0.52 g, 3.1 mmol) in benzene/ethanol (12:1, v/v, 260 mL). The resultant solution was refluxed overnight, affording small crystals, and then concentrated to one-third of its volume; the crystals formed were filtered off, washed with diethyl ether to remove traces of hydriodic acid, and recrystallized from absolute ethanol as well-shaped single crystals. IR (Raman) : ν̃ [cm^{-1}] = 1644 w (1643 m), δ(OH); 1579 m (1583s), 1530 m (1525 w), 1460 vs (1461sh), ν(ring); 1064 s (1061 m), 1015 s (1015 w), ν(CO). ^{13}C CP MAS NMR (see **III** for numbering): δ = 152.5 [C(3)], 143.4 [C(2)], 134.5 [C(6)], 133.2 [C(4)], 131.9 [C(5)], 62.2 [C(7)], 58.4 [C(9)], 47.7 [C(10)], 15.8 [C(8)] ppm. ^{1}H NMR ([D$_6$]DMSO, TMS): δ = 8.43 [s, 1 H, C(6)−H], 5.65 [s, br, 1 H, O(3)−H], 4.80 [s, 2 H, C(9)−H], 4.68 [s, 2 H, C(7)−H], 4.23 [s, 3 H, C(10)−H], 2.59 [s, 3 H, C(8)−H] ppm. ^{13}C{^{1}H} NMR ([D$_6$]DMSO, TMS): δ = 152.6 [C(3)], 144.4 [C(2)], 139.7 [C(6)], 138.2 [C(4)], 134.9 [C(5)], 58.0 [C(7)], 56.5 [C(9)], 46.6 [C(10)], 13.8 [C(8)] ppm.

[MePN]: This compound was prepared from [HMePN]I by reaction with silver carbonate.[23] IR (Raman): ν̃ [cm^{-1}] = 1653 w, δ(OH); 1558 vs (1556 s), 1498 vs (1480 w), 1467 s (1453 m), ν(ring); 1066 m (1066 w), 1020 vs, ν(CO). ^{13}C CP MAS NMR: δ = 161.9 [C(3)], 146.9 [C(2)], 139.2 [C(6)], 134.3 [C(4)], 123.0 [C(5)], 58.4 [C(7)], 53.8 [C(9)], 44.7 [C(10)], 12.1 [C(8)] ppm. ^{1}H NMR ([D$_6$]DMSO, TMS): δ = 7.36 [s, 1 H, C(6)−H], 5.27 [t, ^3J = 5.2 Hz, 1 H, O(3)−H], 4.58 [s, 2 H, C(9)−H], 4.38 [d, 2 H, C(7)−H], 3.95 [s, 3 H, C(10)−H], 2.36 [s, 3 H, C(8)−H] ppm. ^{13}C{^{1}H} NMR ([D$_6$]DMSO, TMS): δ = 165.9 [C(3)], 142.0 [C(2)], 136.8 [C(6)], 134.6 [C(4)], 121.6 [C(5)], 58.8 [C(7)], 58.0 [C(9)], 45.0 [C(10)], 11.9 [C(8)] ppm.

Synthesis of the Complexes

[SnMe$_2$(MePN−H)]I (1): Methyl iodide (8 mL) and solid dimethyltin(IV) oxide (0.51 g, 3.1 mmol) were added to a solution of pyridoxine (0.52 g, 3.1 mmol) in toluene/ethanol (3:1, v/v, 200 mL) and the mixture was refluxed for 24 h. Water was then removed by azeotropic distillation in a Dean−Stark funnel, and the resultant yellow solid was filtered off, washed with diethyl ether and vacuum-dried. Yield 96% (1.36 g). $C_{11}H_{18}INO_3Sn$ (457.9): calcd. C 28.8, H 4.0, N 3.1; found C 28.9, H 4.2, N 3.0. M.p. 205 °C. Λ_M = 57.2 S cm^2 mol^{-1}. The main signals of metallated species in the EI spectrum are at *m*/*z* (%) = 302 (4.1) [Sn(MePN−H)], 150 (30.8) [SnMe$_2$], 135 (28.8) [SnMe] and 120 (46.9) [Sn]. In addition, the EI spectrum shows signals for pyridoxine and its fragments, and the FAB spectrum exhibits signals at *m*/*z* (%) = 664 (43.1) [SnMe$_2$(MePN−H)]$_2$, 332 (100) [SnMe$_2$(MePN−H)] and 302 (10.0) [Sn(MePN−H)]. IR (Raman): ν̃ [cm^{-1}] = 1619 w (1618 w), δ(OH); 1568 m (1568s), 1498 m (1483 w), 1451 s (1450 m), ν(ring); 1067s, 1017 m (1017 w), ν(CO); 587 sh (587 w), ν_{asym}(Sn−C); 518 w (528vs), ν_{sym}(Sn−C); 467 m (461 w), 427 m (425 w), ν(Sn−O). Mössbauer: I.S. = 1.37, Q.S. = 3.20, Γ = 0.92 mm·s^{-1}, $A_{2/1}$ = 1.00. ^{13}C CP MAS NMR: δ = 159.0 [C(3)], 149.0 [C(2)], 143.6 [C(4)], 132.8 [C(6)], 132.8 [C(5)], 60.7 [C(7)], 57.4 [C(9)], 48.4 [C(10)], 16.5 [C(8)], 5.6, 1.8 [C−Sn] ppm. ^{1}H NMR ([D$_6$]DMSO, TMS): δ = 8.05 [s, 1 H, C(6)−H], 5.53 [t, ^3J = 5.2 Hz, 1 H, O(3)−H], 4.89 [s, ^3J(^{1}H-^{119}Sn) = 60.6 Hz, 2 H, C(9)−H], 4.55 [d, ^3J = 5.2 Hz, 2 H, C(7)−H], 4.11 [s, 3 H, C(10)−H], 2.49 [s, 3 H, C(8)−H], 0.58 [s, ^2J(^{1}H-$^{119/117}$Sn) = 87.0/84.4 Hz, 6 H, CH_3−Sn] ppm. ^{13}C{^{1}H} NMR ([D$_6$]DMSO, TMS): δ = 158.9 [C(3)], 145.1 [C(2)], 142.4 [C(4)], 134.9 [C(6)], 130.8 [C(5)], 58.6 [C(7)], 57.9 [C(9)], 45.7 [C(10)], 12.6 [C(8)], 6.1 [^1J(^{13}C-^{119}Sn) = 780.5 Hz, (C−Sn)] ppm. ^{119}Sn NMR {[D$_6$]DMSO, $Sn(CH_3)_4$}: δ = −170.2 ppm. Crystals suitable for X-ray study were obtained by crystallization from methanol.

[SnEt$_2$(MePN−H)]I (2): Methyl iodide (8 mL) and solid diethyltin(IV) oxide (0.59 g, 3.1 mmol) were added to a solution of pyridoxine (0.52 g, 3.1 mmol) in toluene/ethanol (3:1, v/v, 200 mL). After refluxing for 24 h, water was removed by azeotropic distillation in a Dean−Stark funnel and the resultant yellow solid was filtered off and vacuum-dried. Yield 97% (1.46 g). $C_{13}H_{22}INO_3Sn$ (485.9): calcd. C 32.1, H 2.9, N 4.5; found C 32.4, H 2.8, N 4.5. M.p. 239 °C. Λ_M = 73.8 S cm^2 mol^{-1}. The main signals of metallated species in the EI spectrum are at *m*/*z* (%) = 302 (71.5) [Sn(MePN−H)], 178 (10.0) [SnEt$_2$], 149 (36.6) [SnEt] and 120 (30.1) [Sn]. Also, the EI spectrum shows signals for pyridoxine and its fragments, and the FAB spectrum has signals at *m*/*z* (%) = 720 (26.6) [SnEt$_2$(MePN−H)]$_2$, 360 (100) [SnEt$_2$(MePN−H)] and 302 (18.3) [Sn(MePN−H)]. IR (Raman): ν̃ [cm^{-1}] = 1619 w (1618 w), δ(OH); 1564 m (1568s), 1501 w (1500 w), 1455 s (1456 m), ν(ring); 1068 s (1064 w), 1029 m (1033 w), ν(CO); 541 m (545 w), ν_{asym}(Sn−C); 500 w (502 vs), ν_{sym}(Sn−C); 462 m (456 w), 435 m (428 w), ν(Sn−O). Mössbauer: I.S. = 1.49, Q.S. = 3.21, Γ = 0.85 mm·s^{-1}, $A_{2/1}$ = 1.08. ^{13}C CP MAS NMR: δ = 158.9 [C(3)], 147.1 [C(2)], 141.8 [C(4)], 133.9 [C(6)], 133.9 [C(5)], 54.1 [C(7)], 54.1 [C(9)], 46.5 [C(10)], 14.0 [C(8)], 9.7 [C(α)−Sn] ppm. ^{1}H NMR ([D$_6$]DMSO, TMS): δ = 8.07 [s, 1 H, C(6)−H], 5.53 [t, ^3J = 5.2 Hz, 1 H, O(3)−H], 4.91 [s, ^3J(^{1}H-^{119}Sn) = 47.7 Hz, 2 H, C(9)−H], 4.55 [d, ^3J = 5.1 Hz, 2 H, C(7)−H], 4.13 [s, 3 H, C(10)−H], 2.53 [s, 3 H, C(8)−H], 1.29 [m, 4 H, CH(α)−Sn], 1.16 [t, ^3J(^{1}H-$^{119/117}$Sn) = 135.0/128.5 Hz, 6 H, CH(β)−Sn] ppm. ^{13}C{^{1}H} NMR ([D$_6$]DMSO, TMS): δ = 159.3 [C(3)], 144.5 [C(2)], 142.0 [C(4)], 134.7 [C(6)], 130.2 [C(5)], 59.5 [C(7)], 57.7 [C(9)], 45.4 [C(10)], 17.7 [C(β)−Sn], 12.2 [C(8)], 9.6 [C(α)−Sn] ppm. ^{119}Sn NMR {[D$_6$]DMSO, $Sn(CH_3)_4$}: δ = −209.5

ppm. Crystallization from methanol afforded crystals of **2**·2H_2O which were used for X-ray analysis.

[$SnBu_2$(MePN−H)]I (3): Methyl iodide (8 mL) and solid dibutyltin(IV) oxide (0.77 g, 3.1 mmol) were added to a solution of pyridoxine (0.52 g, 3.1 mmol) in toluene/ethanol (3:1, v/v, 200 mL). After refluxing for 24 h, water was removed by azeotropic distillation in a Dean−Stark funnel and the obtained yellow solid was filtered off and vacuum-dried. Yield 98% (1.65 g). $C_{17}H_{30}INO_3Sn$ (542.0): calcd. C 37.7, H 5.6, N 2.6; found C 38.1, H 5.9, N 2.6. M.p. 220 °C. Λ_M = 83.5 S cm^2 mol^{-1}. The main signals of metallated species in the EI spectrum are at *m*/*z* (%) = 302 (12.1) [Sn(MePN−H)], 177 (30.3) [SnBu] and 120 (42.9) [Sn]. Also, the EI spectrum shows signals for pyridoxine and its fragments, and the FAB spectrum exhibits signals at *m*/*z* (%) = 416 (100) [$SnBu_2$(MePN−H)] and 302 (12.1) [Sn(MePN−H)]. IR (Raman): $\tilde{\nu}$ [cm^{-1}] = 1613 w (1612 w), δ(OH); 1565 m (1562 m), 1500 m (1500 w), 1451 s (1443 w), ν(ring); 1063 m (1063 w), 1027 vs (1020 w), ν(CO); 570 m (573 m), ν_{sym}(Sn−C); 461 m, 442 m (450 w), ν(Sn−O). Mössbauer: I.S. = 1.58, Q.S. = 3.49, Γ = 0.77 mm·s^{-1}, $A_{2/1}$ = 1.12. ^{13}C CP MAS NMR: δ = 160.4 [C(3)], 148.2 [C(2)], 140.4 [C(4)], 134.2 [C(6)], 134.0 [C(5)], 61.6 [C(7)], 53.4 [C(9)], 49.1 [C(10)], 14.0 [C(8)], 25.6, 24.3 [C(α)−Sn], 34.4 [C(β)−Sn], 30.1, 28.8 [C(γ)−Sn], 12.8, 11.2 [C(δ)−Sn] ppm. ^{1}H NMR ([D_6]DMSO, TMS): δ = 8.07 [s, 1 H, C(6)−H], 5.54 [t, *J* = 5.0 Hz, 1 H, O(3)−H], 4.92 [s, ^3J(^{1}H-^{119}Sn) = 56.8 Hz, 2 H, C(9)−H], 4.55 [d, *J* = 5.2 Hz, 2 H, C(7)−H], 4.13 [s, 3 H, C(10)−H], 2.51 [s, 3 H, C(8)−H], 1.30 [t, 4 H, CH(α)−Sn], 1.54 [q, ^2J(^{1}H-^{119}Sn) = 85.7 Hz, 4 H, CH(β)−Sn], 1.29 [m, ^3J(^{1}H-^{119}Sn) = 93.0 Hz, 4 H, CH(γ)−Sn], 0.82 [t, 6 H, CH(δ)−Sn] ppm. ^{13}C{^{1}H} NMR ([D_6]DMSO, TMS): δ = 159.3 [C(3)], 144.5 [C(2)], 142.5 [C(4)], 135.0 [C(6)], 130.5 [C(5)], 60.0 [C(7)], 57.8 [C(9)], 45.7 [C(10)], 12.4 [C(8)], 23.9, ^1J(^{13}C-^{119}Sn) = 660.0 Hz, [C(α)−Sn], 26.9 [C(β)−Sn], 25.9 [C(γ)−Sn], 13.5 [C(δ)−Sn] ppm. ^{119}Sn NMR {[D_6]DMSO, $Sn(CH_3)_4$}: δ = −190.9 ppm.

[$SnPh_2$(MePN−H)]I·H_2O (4): Methyl iodide (8 mL) and solid diphenyltin oxide (0.90 g, 3.1 mmol) were added to a solution of pyridoxine (0.52 g, 3.1 mmol) in toluene/ethanol (3:1, v/v, 200 mL). After refluxing for 24 h, water was removed by azeotropic distillation in a Dean−Stark funnel and the resultant yellow solid was filtered off and vacuum-dried. Yield 90% (1.67 g). $C_{21}H_{22}INO_3Sn·H_2O$ (600.0): calcd. C 42.0, H 4.0, N 2.3; found C 41.6, H 4.1, N 2.6. M.p. > 250 °C. Λ_M = 70.8 S cm^2 mol^{-1}. The main signals of metallated species in the EI spectrum are at *m*/*z* (%) = 348 (72.6) [SnPh(PN−2H)], 197 (71.4) [SnPh] and 120 (55.8) [Sn]. Also, the EI spectrum shows signals for pyridoxine and its fragments, and the FAB spectrum shows signals at *m*/*z* (%) = 455 (8.8) [$SnPh_2$(MePN−H)], 302 (100) [Sn(MePN−H)], 286 (5.7) [Sn(PN−2H)], 274 (5.4) [$SnPh_2$], 197 (24.8) [SnPh] and 120 (12.2) [Sn]. IR (Raman): $\tilde{\nu}$ [cm^{-1}] = 3333 br, ν(OH); 1614 w (1614 w), δ(OH); 1562 w (1576 m), 1493 w, 1479 w (1477 w), 1450 s (1447 w), ν(ring); 1020 m (1022 m), 997 m (998 vs), ν(CO); 443 w (444 w), ν(Sn−O); 270 m (270 w), ν_{asym}(Sn−C); 233 m (230 w), ν_{sym}(Sn−C). Mössbauer: I.S. = 1.44, Q.S. = 2.87, Γ = 0.83 mm·s^{-1}, $A_{2/1}$ = 1.09. ^{1}H NMR ([D_6]DMSO, TMS): δ = 7.99 [s, 1 H, C(6)−H], 5.50 [s, br, 1 H, O(3)−H], 4.81 [s, 2 H, C(9)−H], 4.51 [s, br, 2 H, C(7)−H], 4.10 [s, 3 H, C(10)−H], 2.50 [s, 3 H, C(8)−H], 7.79 [d, ^3J = 7.3 Hz, 4 H, CH_o−Sn], 7.57 [s, 4 H, CH_m−Sn], 7.55 [s, 2 H, CH_p−Sn] ppm. ^{13}C{^{1}H} NMR ([D_6]DMSO, TMS): δ = 159.9 [C(3)], 140.0 [C(2)], (not observed) [C(4)], 135.1 [C(6)], 128.3

Table 2. Crystal data, data collection and structure refinement parameters

	[HMePN]I	**1**	**2**·H_2O	**3**
Empirical formula	$C_9H_{14}INO_3$	$C_{22}H_{36}I_2N_2O_6Sn_2$	$C_{26}H_{52}I_2N_2O_{10}Sn_2$	$C_{34}H_{60}I_2N_2O_6Sn_2$
Formula mass	311.11	915.71	1043.88	1084.02
Wavelength [Å]	1.54184	0.71073	0.71073	0.71073
Crystal system	monoclinic	monoclinic	monoclinic	tetragonal
Space group	$P2_1/n$ (no. 14)	$P2_1/c$ (no. 14)	$P2_1/c$ (no.14)	$I4_1/a$ (no. 88)
Unit-cell dimensions				
a [Å]	6.6014(6)	6.8596(8)	9.5030(12)	27.298(7)
b [Å]	11.4994(10)	12.136(2)	13.5203(10)	27.298(7)
c [Å]	14.9980(17)	18.833(8)	15.465(2)	11.738(4)
β [°]	98.129(12)	93.709(11)	107.651(14)	
V [Å^3]	1127.09(19)	1564.6(8)	1893.4(4)	8747(4)
Z	4	2	2	8
$D_{calcd.}$ [Mg·m^{-3}]	1.833	1.944	1.831	1.646
F(000)	608	872	1016	4256
μ [mm^{-1}]	22.218	3.604	2.997	2.592
Crystal size [mm]	0.25 × 0.25 × 0.15	0.25 × 0.15 × 0.10	0.20 × 0.20 × 0.20	0.35 × 0.25 × 0.10
θ range for data collection [°]	4.86−74.26	3.36−26.18	2.25−26.29	2.11−28.44
θ range (25 reflect.) [°]	14.377 < θ <42.678	9.327 < θ < 20.876	8.674 < θ < 18.086	11.882 < θ < 12.563
Index ranges	$0 \le h \le 8$	$0 \le h \le 8$	$0 \le h \le 11$	$-36 \le h \le 0$
	$-14 \le k \le 14$	$-15 \le k \le 0$	$0 \le k \le 16$	$0 \le k \le 36$
	$-18 \le l \le 18$	$-23 \le l \le 23$	$-19 \le l \le 18$	$-15 \le l \le 0$
Reflections collected	4884	3406	4072	5730
Unique reflections	2305 (R_{int} = 0.0523)	3138 (R_{int} = 0.0948)	3839 (R_{int} = 0.0283)	5503 (R_{int} = 0.0757)
Absorption correction	ψ-scan	ψ-scan	ψ-scan	ψ-scan
Max., min. transmission	0.983, 0.569	0.946, 0.790	0.975, 0.947	0.980, 0.895
Data, restraints, parameters	2305, 0, 129	3138, 0, 154	3839, 0, 264	5503, 0, 208
Goodness of fit on F^2	1.007	0.890	1.014	0.970
Final *R* indices [$I > 2\sigma(I)$]	R_1 = 0.0675, wR_2 = 0.1812	R_1 = 0.0815, wR_2 = 0.1302	R_1 = 0.0380, wR_2 = 0.0850	R_1 = 0.0514, wR_2 = 0.1205
R indices (all data)	R_1 = 0.0863, wR_2 = 0.1998	R_1 = 0.2561, wR_2 = 0.1721	R_1 = 0.0897, wR_2 = 0.0981	R_1 = 0.1957, wR_2 = 0.1558
Largest peak, hole difference [e·Å^{-3}]	2.273, −1.862	0.947, −1.14 0	1.373, −0.932	1.264, −1.153

[C(5)], 59.6 [C(7)], 57.9 [C(9)], 45.5 [C(10)], 12.4 [C(8)], 144.2 (C_i−Sn), 136.0 (^2J = 46.8 Hz, C_o−Sn), 130.2 (C_m−Sn), 129.1 (C_p−Sn) ppm. ^{119}Sn NMR {[D_6]DMSO, $Sn(CH_3)_4$}: δ = −233.5 ppm.

Crystal Structure Determination

X-ray Data Collection and Reduction: Crystals were mounted on glass fibres for data collection with Enraf−Nonius automatic diffractometers (a CAD4 for [HMePN]I and a MACH3 for **1**, **2**·2H_2O and **3**).[24] Cell constants and an orientation matrix for data collection were calculated by least-squares refinement of the diffraction data for 25 reflections. Data were collected at 293 K by the ω-scan technique using Cu-K_α radiation (λ= 1.54184 Å) for [HMePN]I and Mo-K_α radiation (λ= 0.71073 Å) for **1**, **2**·2H_2O and **3**, and were corrected for Lorentz and polarization effects.[25] Semiempirical absorption corrections (ψ-scan) were also made.[26]

Structure Solution and Refinement: The structure was solved by direct methods[27] and subsequent Fourier maps, and was refined on F^2 by a full-matrix least-squares procedure using anisotropic displacement parameters.[28] Hydrogen atoms were placed at calculated positions (C−H 0.93−0.97 Å) and refined using a riding model. Atomic scattering factors were taken from ref.[29] Molecular graphics were generated with PLATON.[30] The crystal data, experimental details and refinement results are summarized in Table 2.

CCDC-187692 for [HMePN]I, -187693 for [$SnMe_2$(MePN−H)]I, -187694 for [$SnEt_2$(MePN−H)]I·2H_2O and -187695 for [$SnBu_2$(MePN−H)]I contain the supplementary crystallographic data for this paper. These data can be obtained free of charge at www.ccdc.cam.ac.uk/conts/retrieving.html [or from the Cambridge Crystallographic Data Centre, 12 Union Road, Cambridge CB2 1EZ, UK; Fax: (internat.) + 44-1223/336-033; E-mail: deposit@ccdc.cam.ac.uk].

Acknowledgments

We thank the Xunta de Galicia, Spain, for financial support under Project XUGA 20316 B94. F. C. thanks the Spanish Agency for International Cooperation and the University of Santiago de Compostela for grants.

[1] J. S. Casas, M. V. Castaño, M. S. García-Tasende, T. Perez Alvarez, A. Sánchez, J. Sordo, *J. Inorg. Biochem.* **1996**, *61*, 97.
[2] [2a] J. S. Casas, A. Castiñeiras, M. D. Couce, G. Martinez, J. Sordo, J. M. Varela, *J. Organomet. Chem.* **1996**, *517*, 165. [2b] J. S. Casas, E. E. Castellano, M. D. Couce, M. S. García-Tasende, A. Sánchez, J. Sordo, C. Taboada, E. M. Vázquez-López, *Inorg. Chem.* **2001**, *40*, 946.
[3] J. S. Casas, E. E. Castellano, F. Condori, M. D. Couce, A. Sánchez, J. Sordo, J. M. Varela, J. Zuckerman-Schpector, *J. Chem. Soc., Dalton Trans.* **1997**, 4421.
[4] J. S. Casas, A. Castiñeiras, F. Condori, M. D. Couce, U. Russo, A. Sánchez, J. Sordo, J. M. Varela, *Polyhedron* **2000**, *19*, 813.
[5] W. Korytnyk, in *Vitamin B_6 Pyridoxal Phosphate* (Eds.: D. Dolphin, P. Pouloon, O. Avramovich), Wiley, New York, **1986**, part A, p.371.
[6] K. Wada, S. Ishigaki, K. Veda, J. Take, K. Sasaki, M. Sakata, M. Haga, *Chem. Pharm. Bull.* **1988**, *36*, 1779.
[7] [7a] M. Gielen, R. Willem, T. Mancilla, J. Ramharter, E. Joosen, *Silicon, Germanium, Tin Lead Compd.* **1986**, *9*, 349. [7b] F. Kayser, M. Biesemans, M. Gielen, R. Willlem, *Main Group Met. Chem.* **1994**, *17*, 559. [7c] F. Kayser, M. Biesemans, M. Gielen, R. Willem, *Magn. Res. Chem.* **1994**, *32*, 358.
[8] J. Longo, K. J. Franklin, M. F. Richardson, *Acta Crystallogr., Sect. B* **1982**, *38*, 2721.
[9] G. E. Bacon, J. S. Plant, *Acta Crystallogr., Sect. B* **1980**, *36*, 1130.
[10] A. W. Addison, T. N. Rao, J. Reedijk, J. Van Rijn, G. C. Verschoov, *J. Chem. Soc., Dalton Trans.* **1984**, 1349.
[11] J. E. Huheey, E. A. Keiter, R. L. Keiter, *Inorganic Chemistry. Principles of Structure and Reactivity*, 4th ed., Harper Collins College Publishers, New York, **1993**, p. 292.
[12] C. E. Holloway, M. Melnik, *Main Group Met. Chem.* **2000**, *23*, 331.
[13] N. A. Drobinskaya, L. V. Inova, M. Ya Karpeiskii, V. L. Florent'er, *Chem. Heterocycl. Compd. (Engl. Trans.)* **1973**, *7*, 330.
[14] H. L. Sing, A. K Varshney, *Main Group Met. Chem.* **1999**, *22*, 529.
[15] R. V. Parish, "Structure and Bonding in Tin Compounds", in G. L. Long (Ed.) *Mössbauer Spectroscopy Applied to Inorganic Chemistry*, Plenum, New York, **1984**.
[16] T. P. Lockhart, W. F. Manders, *Inorg. Chem.* **1986**, *25*, 892.
[17] C. Pettinari, F. Marchetti, A. Cingolani, A. Gindulyte, L. Massa, M. Rossi, F. Caruso, *Eur. J. Inorg. Chem.* **2001**, 2171.
[18] T. P. Lockhart, W. F. Manders, *J. Am. Chem. Soc.* **1987**, *109*, 7015.
[19] J. Holecek, A. Lycka, *Inorg. Chim. Acta* **1986**, *118*, L15.
[20] R. K. Harris, J. D. Kennedy, W. McFarlane, in R. K. Harris, B. E. Mann (Eds.), *NMR and the Periodic Table*, Academic Press, London, **1978**, p. 342.
[21] J. Otera, *J. Organomet. Chem.* **1981**, *221*, 57.
[22] J. Holecek, M. Nádvorník, K. Handlír, A. Lycka, *J. Organomet. Chem.* **1986**, *315*, 299.
[23] S. A. Harris, T. J. Webb, K. Folkers, *J. Am. Chem. Soc.* **1940**, *62*, 3198.
[24] B. V. Nonius, *CAD4-Express Software*, version 5.1/1.2, Enraf−Nonius, Delft, The Netherlands, **1994**.
[25] M. Kretschmar, *GENHKL, Program for the reduction of CAD4 diffractometer data*, University of Tübingen, Germany, **1997**.
[26] A. C. T. North, D. C. Phillips, F. S. Mathews, *Acta Crystallogr., Sect. A* **1968**, *24*, 351.
[27] G. M. Sheldrick, *Acta Crystallogr., Sect. A* **1990**, *46*, 467.
[28] G. M. Sheldrick, *SHELXL-97, Program for the refinement of crystal structures*, University of Göttingen, Germany, **1997**.
[29] *International tables for crystallography*, Kluwer Academic Publishers, Dordrecht, The Netherlands, **1995**, vol. C.
[30] A. L. Spek, *PLATON, A Multipurpose Crystallographic Tool*, University of Utrecht, The Netherlands, **1997**.

Received November 15, 2002

